PROCEEDINGS OF SCIENCE

Direct breakup reaction of ^{8}B at Fermi energy

Jian-Song Wang[1]*, Shi-Lun Jin§, Yan-Yun Yang, Zhen Bai, Jun-Bing Ma, Peng Ma, Xin-Quan Liu, Wei-Hu Ma, Zhi-Hao Gao, Qiang Hu
Institute of Modern Physics, Chinese Academy of Sciences
509 Nanchang Road, Lanzhou, China
E-mail: jswang@impcas.ac.cn; §jinshilun@impcas.ac.cn;*

Cheng-Jian Lin, Xin-Xing Xu
Institute of Nuclear Physics, China Institute of Atomic Energy
Beijing 100049, China

The longitudinal momentum distributions of the core-like fragment ^{7}Be from the breakup of ^{8}B on ^{12}C target have measured at the energy of 36MeV/u at the Radioactive Ion Beam Line in Lanzhou (RIBLL). In order to distinguish the stripping and diffraction mechanisms involving in breakup reaction of ^{8}B, both fragments of ^{7}Be and proton are measured coincidently. With this coincident measurement, the widths of longitudinal momentum distribution are deduced with the values of 124±17MeV and 92±7 MeV for stripping and diffraction mechanism respectively. It is found that the longitudinal momentum width of stripping component is larger than that of diffraction component, which is different from the breakup reaction at high energy as around GeV/u. The theoretical calculations are compared with these experimental results.

The 26th International Nuclear Physics Conference
11-16 September, 2016
Adelaide, Australia

[1]Speaker

PoS(INPC2016)199

1. Introduction

The halo structure is one of the most interesting phenomena since the radioactive beam facilities were developed to study the structure of unstable nuclei close to the dripline in 1980s. Many neutron-halo nuclei are discovered, such as ^{6}He, ^{11}Li, ^{11}Be, ^{14}Be ^{17}B, ^{19}C and only three proton-halo nuclei are experimentally observed, namely ^{8}B, ^{12}N and ^{17}Ne [1, 2]. A typical characteristic of halo structure is one or more valence nucleons surrounding a tightly bound core nucleus very extensively due to the loosely bound of the valence nucleons [3]. The enhanced total reaction cross section and a narrow width of the longitudinal momentum distribution of the core-like fragment are usually regarded as the experimental signatures of the halo structure.

^{8}B is a proton-drip nucleus with a smallest separation energy of 134keV for the last proton. It has attracted intense experimental and theoretical attentions because of the exotic structure and its astrophysical significance [4-12]. The enhanced total reaction cross sections have been measured and the theoretical analysis based on them indicates a quite significant extension of the last proton beyond that of the core, at least a weakly developed proton halo or skin due to the Coulomb and centrifugal potential [13-17]. A quite large quadruple moment was measured for ^{8}B in Ref. [18]. However it could be partly contributed by the very distortable ^{7}Be core [19]. There are also many experiments performed to measure the longitudinal momentum distributions with the energy from several tens MeV/u to several GeV/u [17, 20-23]. The Full Width at Half Maximum (FWHMs) of the longitudinal momentum distributions are relatively narrow. Ref. [23] give a much narrower FWHM of the longitudinal momentum distribution as 81±4MeV/c at the energy of 41 MeV/u. The authors make a conclusion, in the help of a theoretical model calculations, that it is not necessary to assume an unusually extended spatial distribution of the last proton to explain the narrow width and the breakup mechanisms alter the connection between halo size and momentum distribution width. However, they do not distinguish the different mechanisms experimentally.

In this talk, we will give the recently experimental results in which the different breakup mechanisms are experimentally distinguished using a coincident measurement as same as the method used in Ref. [24].

2. Experiment and data analysis

2.1 Experimental setup

The Radioactive Ion Beam Line in Lanzhou (RIBLL) was built at Institute of Modern Physics in 1997 [25]. It consists of 4 dipole magnets and 16 qudrapole magnets with the structure of two doubley acromatic parts (see figure.1 for the schematic diagram). The ^{8}B beams were produced by RIBLL with a primary beam of 80.1MeV/u ^{12}C with the beam intensity about 300enA. The production target was a ^{9}Be metal with a thickness of 4171 μ m. An aluminum degrader with a thickness 1112 μ m is placed at the fisrt focal plane (C1) to reduce the contaminated beams of ^{9}C, ^{7}Be and ^{6}Li. The secondary beams were identified by a 17m time of flight, energy loss detector and a certain magnetic rigidity setting.

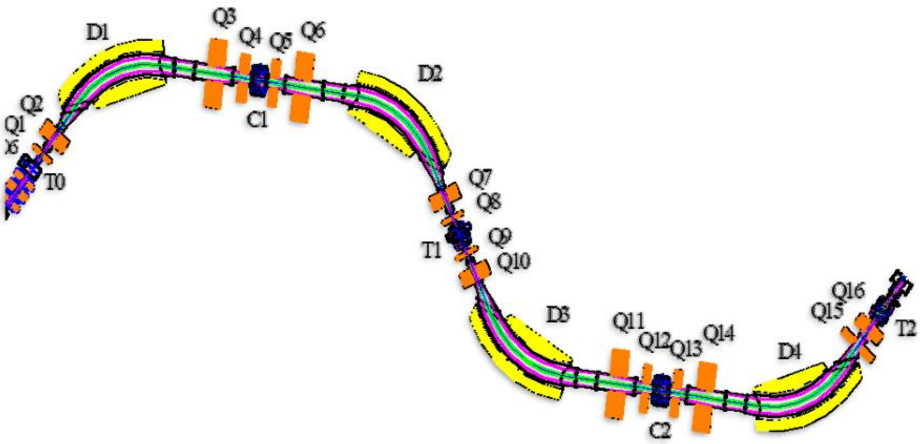

Figure 1: Schematic digram of RIBLL

Our detectors were set up at the sencond focal point (T2) of RIBLL. Two Parallel-Plate Avalanch Counters with a distance of 480mm were placed before the reaction target, a self-supported carbon foil with a thichness of 45 mg/cm^2, to record the tracks of incoming beams. A double-sided silicon strip detector and a 64-unit CsI(Tl) array composed a dE-E telescope array which covered the polar angle from -17^o to 17^o in the experimental frame. The Figure 2 is a photo of the experimental setup. The more details bout the experimental setup are described in the published paper [26].

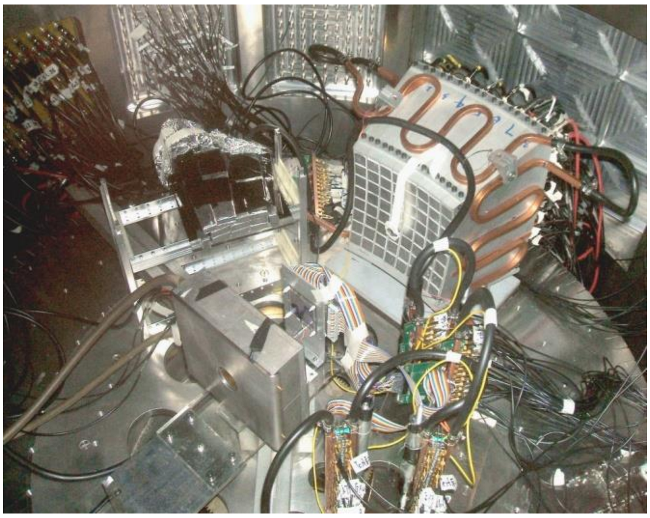

Figure 2: The photo of experimental setup.

2.2 Data analysis

Figure 3(a) shows the dE-E spectrum measured by the dE-E telescope array. It can be seen clearly that the unreacted cocktail beams dominate on this spetrum because our detector covered zero degree. The particle identifications are indicated in the figure. Because the charged particle with a larger ratio of mass over charge has a smaller velocity at the same magnetic rigidity, the velocities of ^{8}B and ^{9}C are larger than that of ^{7}Be. In the breakup reaction, the fragments move with the velocity around the projectile velocity. So the ^{7}Be fragment from breakup of ^{8}B and ^{9}C have a larger velocity than the contaminated beam ^{7}Be. So it is easy to select the breakup events. The events in the red solid rectangle correpond the ^{7}Be fragments from breakup of ^{8}B and ^{9}C. In order to select the events of ^{8}B breakup reactions, a window is put on the time of flight spectrum (Figure3b). The distance of flight is from T1 to T2 at RIBLL, where two thin plastic scintillator were used as timing detectors.

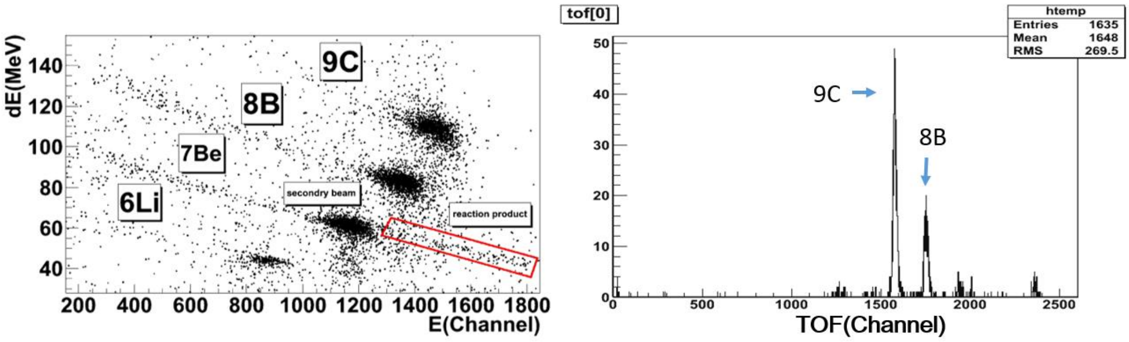

Figure 3: (Left) dE-E 2 dimension spectrum to identify the charged particles and select the reaction events. The events in the red frame are the ^{7}Be fragment from the breakup of ^{8}B and ^{9}C. (Right) The time of flight (TOF) of the sencondary beams, ^{9}C, ^{8}B and other contaminations. A window is put on ^{8}B to select the breakup events with the coicidently measured proton.

The sum energy of ^{7}Be fragment and proton were reconsttructed event by event. As shown in Figure 4, a sharp peak located around 275MeV correponds to the diffraction breakup in which the total kinetic energy of ^{8}B system is conserved after breaking up. While a relative broad peak laocted at lower energy corresponds to the stripping breakup in which a part of total kinetic energy was lost to excite the target nucleus or the fragments. This method is demonstrated in Ref. [24] to be an effective means to distinguish the diffraction and stripping mechanisms of breakup reaction.

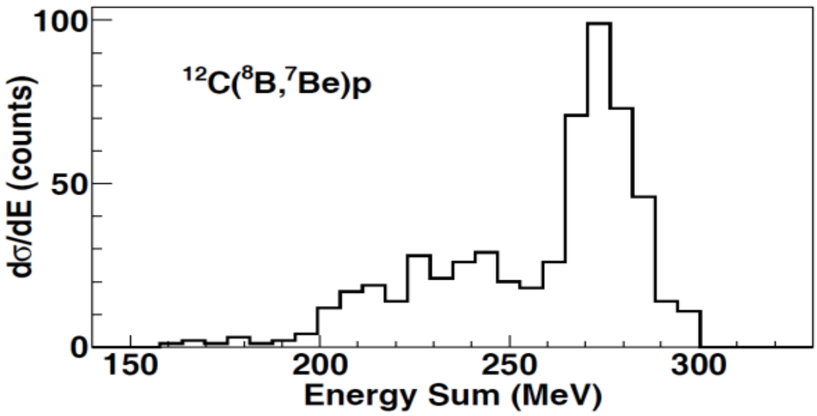

Figure 4: Energy sum spectrum of the ^{7}Be and proton from the breakup of ^{8}B. The sharp peak at the energy about 275MeV represent the events from diffraction mechanism and the broad one at lower energy is from the stripping mechanism.

The logitudinal momentum distributions of ^{7}Be fragment from stripping (Figure 5a) and diffraction (Figure 5b) mechanisms are deduced respectively using the above method. The solid lines are the fitting with a Lorentz function. In Figure 5a, two different fittings are employed to the logitudinal momentum distribution of the stripping component. It looks that a bunch of fittings could applied to it with very different widths due to the low statatistics. So we take a compromised value of width, 124±17MeV, with a relative large system error bar. For the diffraction component, a width of 92±7 MeV is obtained by Lorentz fitting as shown in Figure 5b.

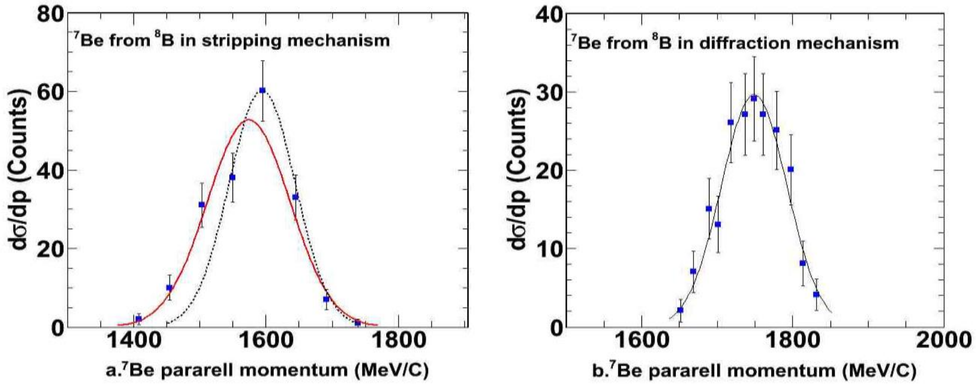

Figure 5: the logitudinal momentum distributions for stripping micahnism (left) and differaction mechanism (right). The solid lines are the fitting to get the widths.

3. Results and discussion

The effective three-body model calculations and Continuum Discretized Coupled-Channels calculations, performed by J. A. Tostevin, are compared with the experimental data in Figure 6 and Figure 7.

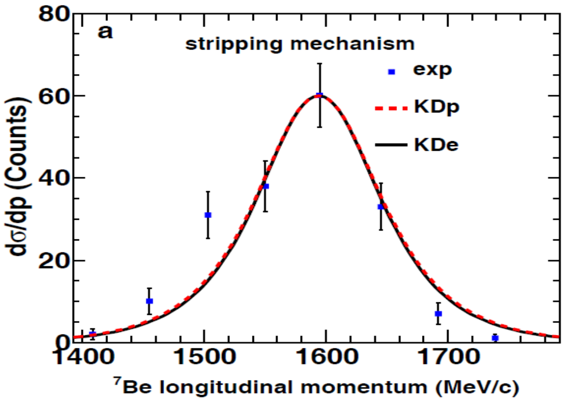

Figure 6: (Color online) The logitudinal moemntum of ^7Be fragments from the the stripping breakup of ^8B on a carbon target. The blue solid points with error bar represent the experimental data. The red dahsed line and black solid line are the effectvie three-body model calculations with KDp and KDe potential. (see the text for detail)

The complex ^7Be-target optical potential was calculated using the double-folding method in Ref. [27], assuming the Gaussian density distributions of ^7Be and ^{12}C with rms radii 2.31fm and 2.32fm. The proton-target potential was calculated from the Koning and Delaroche global parameterization [28]. The solid line in Figure 6 is the calculations using the eikonal approximation formalism [29] and the eikonal phase shifts and S-matrices of the above potentials (denoted KDe). Due to the relatively low beam energy, calculations were repeated using the improved description of the proton-target S-matrix (denoted KDp) which just give a slight difference. These calculations can reproduce the experimental data although it is not perfect because the theoretical treatment of stripping mechanism is not easy, especially for this low energy region. On the other hand, the error bar of the experimental data is large and the statistics is also not good enough. The more accuracy measurements are expected.

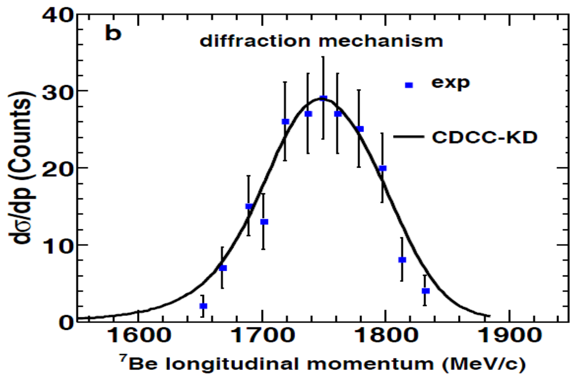

Figure 7: (Color online) The logitudinal moemntum of ^{7}Be fragments from diffractive breakup of ^{8}B on a carbon target. The blue solid points with error bar represent the experimental data. The CDCC calculations with KD potential are shown with a black solid line.

The diffraction logitudinal momentum distributions, shown in Figure 7, can be well discribed by the CDCC calculations in a breakup model space [24].

In a summary, the logitudinal momentum distributions of ^{7}Be fragments from the stripping and diffraction mechanism of breakup of ^{8}B on a carbon target at 36MeV/u are measured with a coicident method at RIBLL. The experimental data show a marginal difference of the logitudinal momentum distributions between stripping and diffraction. The theoretical calculations show the same tendency.

This work is supported partly by the National Natural Science Foundation of China (U1432247, 11075190) and the National Basic Research Program of China (973 Program, 2014CB845405).

References

[1] Isao Tanihata, *J. Phys. G* **22** (1996) 157.

[2] Isao Tanihata *et al.*, *Progress in Particle and Nuclear Physics*, **68** (2013) 215.

[3] P. G. Hansen and B. Johson, *EuroPhys. Lett.* **4** (1987) 409.

[4] T. Motobayashi *et al.*, *Phys. Rev. Lett.* **73**(1994)2680.

[5] B. Davids *et al.*, *Phys. Rev. Lett.* **81** (1998) 2019.

[6] N. Iwasa *et al.*, *Phys. Rev. Lett.* **83** (1999) 2910.

[7] B. Davids *et al.*, *Phys. Rev. Lett.* **86** (2001) 2750.

[8] F. Schumann *et al.*, *Phys. Rev. Lett*. **90** (2003) 232501.

[9] Weiping Liu *et al.*, *Phys. Rev. Lett.* **77** (1996) 611.

[10] F. Hammache *et al.*, *Phys. Rev. Lett.* **86** (2001) 3985.

[11] R. Junghans *et al., Phys. Rev. Lett.* **88** (2002) 041101.

[12] L.T. Baby *et al., Phys. Rev. Lett.* **90** (2003) 022501.

[13] I. Tanihata *et al., Phys. Lett. B* **206** (1988) 592.

[14] J. S. Al-Khalili and J. A. Tostevin, *Phys. Rev. Lett.* **76** (1996) 3903.

[15] R.E. Warner *et al., Phys. Rev. C* **52** (1995) R1166.

[16] Quan-Jin Wang *et al., Progress in Natural and Science,* **16** (2002) 29 in Chinese.

[17] F. Negoita *et al., Phys. Rev. C* **54** (1996) 1787.

[18] T. Minamisono *et al., Phys. Rev. Lett.* **69** (1992) 2058.

[19] Attila Csótó, *Phys. Lett. B* **315** (1993) 24.

[20] W. Schwab *et al., Z. Phys. A* **350** (1995) 283.

[21] M. H. Smedberg *et al., Phys. Lett. B* **452** (1999) 1.

[22] D. Cortina-Gil *et al., Phys. Lett. B* **529** (2002) 36.

[23] J. H. Kelley *et al., Phys. Rev. Lett.* **77** (1996) 5020.

[24] D.Bazin *et al., Phys. Rev. Lett.* **102** (2009) 232501.

[25] Wenlong Zhan *et al., Science in China* **42** (1999) 528.

[26] S.L.Jin *et al., Phys. Rev. C* **91** (2015) 054617.

[27] J. A. Tostevin *et al., Phys. Rev. C* **74** (2006) 064604.

[28] A. J. Koning *et al., Nucl. Phys. A* **713** (2003) 231.

[29] C. A. Bertulani *et al., Phys. Rev. C* **70** (2004) 034609.